CIRP Annals - Manufacturing Technology 74 (2025) 239–243

Contents lists available at ScienceDirect

CIRP Annals - Manufacturing Technology

journal homepage: https://www.editorialmanager.com/CIRP/default.aspx

Spatially resolved wire EDM discharge analysis for dynamic part strength evaluation

Andreas Klink (2)[a,*], Lukas Welschof[a], Kai Oßwald[b], Tim Herrig[a]

[a] Manufacturing Technology Institute (MTI) of RWTH Aachen University, Aachen, Germany
[b] Pforzheim University, Pforzheim, Germany

ARTICLE INFO

Article history:
Available online 19 May 2025

Keywords:
Wire EDM
Monitoring
Bending fatigue

ABSTRACT

Wire Electrical Discharge Machining (Wire EDM) is particularly suitable for producing high-precision geometries in demanding materials such as the manufacture of profile grooves in turbine disks. Advanced monitoring nowadays allows the time and spatially resolved in-process discharge analysis. Therefore, in this paper the machining of Inconel 718 parts is fundamentally studied and the resulting surface integrity in terms of roughness and residual stresses is evaluated for main and trim cut strategies. Finally, the resulting bending fatigue performance is characterized in a zone resolved and overall averaged analysis along the workpiece height and compared to reference results of alternative machining approaches.
© 2025 The Authors. Published by Elsevier Ltd on behalf of CIRP. This is an open access article under the CC BY license (http://creativecommons.org/licenses/by/4.0/)

1. Introduction

Wire Electrical Discharge Machining (Wire EDM) allows the realization of highly precise geometries in parts independent of their mechanical properties. Besides the industrially well-known machining of hardened tool steel in the die and mold industry it became particularly interesting for the machining of high strength and difficult-to-cut materials in the turbomachinery sector [1,2]. Especially, for the realization of profile grooves (fir tree slots) in turbine discs out of demanding nickel-based alloys, Wire EDM proved to be a viable alternative manufacturing process. This has been exemplarily shown both from technological and economical point of view [3,4].

Nevertheless, as Wire EDM relies on a thermal material removal and is therefore inherently connected to a correspondingly influenced rim zone, the individual process- and material-specific characteristics of the surface integrity are of eminent interest. To allow a technological comparison to alternative manufacturing technologies like milling, broaching or grinding, this can only be realized by evaluating the resulting dynamic part strength.

Important early work – at least in CIRP – dates to 2008 where Aspinwall et al. [5] investigated the surface integrity after Wire EDM of Ti6Al4V and Inconel 718 with advanced minimum damage generator technology first. Subsequently, Antar et al. [6] could successfully show comparable levels of Wire EDM finished and milled parts in four-point bending fatigue tests.

Welling [7] analysed an application-driven two-trim cut Wire EDM strategy for Inconel 718 both from technological and economic points of view compared to broaching and grinding. He could show that the derived EDM technology achieved the same level of high cycle bending fatigue compared to an industrially defined broaching operation. Only grinding achieved higher values. Ayesta et al. [8] additionally analysed the low cycle fatigue behaviour and they could show that no significant differences remained comparing Wire EDM and grinding for their setup.

Chen et al. [9] finally executed a four-point bending test comparing Wire EDM with polished samples. Here, due to the best surface integrity achieved by polishing, the EDM results showed 30% less fatigue strength. Holmberg et al. [10] derived regression models regarding the influences of roughness and residual stresses on fatigue life in their technology comparison. In the process setup Wire EDM (only rough machining for achieving highest cutting speed) achieved the lowest values due to highest surface roughness and tensile residual stresses compared to milling and abrasive water jet machining.

To remove the thermally influenced layer of Wire EDM for fir tree profile applications, post-processes were studied. Van Riel et al. [11] analysed the capabilities of Wire Electro Chemical Machining (Wire ECM) to finish specimens after being machined by Wire EDM on the same machine tool. The precise EDM contour from the first cut allowed an ECM trim cut maintaining accuracy and smoothing of the surface roughness. However, this was executed for stainless steel. Pure Wire ECM, investigated by the authors [12] in contrast could not achieve the precision level of Wire EDM when applying a single roughing operation.

In industrial process chains, typically a shot peening process is executed to generate compressive residual surfaces stresses in the profiles. Therefore, Küpper et al. [13] studied in detail the surface integrity aspects of broaching, grinding, Wire EDM and ECM after shot peening of Inconel 718. Thermal and thermo-mechanical rim zones were completely removed and compressive stresses introduced without any apparent remaining influence of the subtractive processes. Finally, the authors [14] conducted bending fatigue performance tests for similar roughing-finishing sequences and post-processing confirming its positive effects.

* Corresponding author.
E-mail address: a.klink@mti.rwth-aachen.de (A. Klink).

https://doi.org/10.1016/j.cirp.2025.04.076
0007-8506/© 2025 The Authors. Published by Elsevier Ltd on behalf of CIRP. This is an open access article under the CC BY license (http://creativecommons.org/licenses/by/4.0/)

Besides the time resolved analysis of EDM processes, recent advanced process monitoring approaches in Wire EDM also allow the spatially resolved evaluation along the part height. Boccadoro et al. [15] exemplarily showed the successful industrial implementation. Küpper et al. [16] derived corresponding heat maps regarding the discharge distribution. This finally allowed Küpper et al. [17] to successfully forecast workpiece curvature only based on measured process data during the main cut. In a final step, this procedure was enlarged to a purely data-driven machine learning approach for better generalizability [18].

Therefore, based on advanced local process data measurements, this paper analyses spatially resolved Wire EDM influence on the resulting surface roughness and residual stress distribution for machining of Inconel 718. Generator settings of main and two trim cuts are distinctly varied and the resulting bending fatigue performance is evaluated and benchmarked.

2. Experimental setup and boundary conditions

All experimental trials were carried out on a GFMS Cut P550 Wire EDM machine tool in a water-based dielectric. A brass wire electrode with gamma-phase-brass coating with a diameter of 0.25 mm was used as tool. Based on the machine's standard parameter set a main and two trim cuts were optimized for achieving a roughness value of Ra ≈ 0.8 µm on Inconel 718.

To achieve a zone-based spatial resolution concerning the dynamic strength four individual specimen ($5 \times 55 \times 10$ mm^3) were stacked, Fig. 1. This resulted in an effective workpiece height of 40 mm and flushing conditions with 15 mm nozzle distance [19]. The part height is comparable to typical fir tree slots and by the segmentation, a zone resolved analysis becomes possible. Machining of 1 mm depth over a length of 25 mm was implemented from both sides. For the dynamic tests notches were machined into the individual specimens, using extremely gentle Wire EDM parameter sets. A specimen width of 5 mm remained.

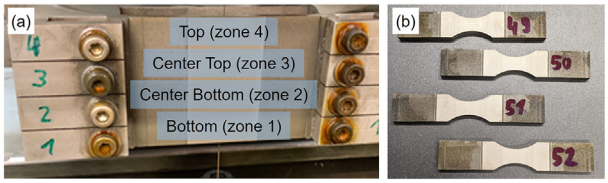

Fig. 1. Wire-EDM clamping (a) and individual finished test parts (b).

A data acquisition unit served to capture the electrical signals of each individual discharge at a high sample rate of at least 100 MHz. The current signals were acquired at both, the upper and lower wire contact. The current difference was used to calculate the discharge location along the height.

To investigate the influence of the process parameters five basic sets of different manufacturing sequences were designed. Fig. 2 depicts this systematic approach. The variations concern different values for the discharge energy W_e for the main cut (by varying discharge current i_e and pause duration t_0) and the first trim cut, respectively. For the second trim cut the discharge frequency f_e was varied as well as the base voltage U_{base} parameter of the specific machine control. The result is five parameter sets for experimental series named E1 (E1T) to E5.

To determine the influence of the process on the dynamic part strength the specimens were finally tested for bending fatigue strength (according to DIN 50,100). The test cycle was designed to

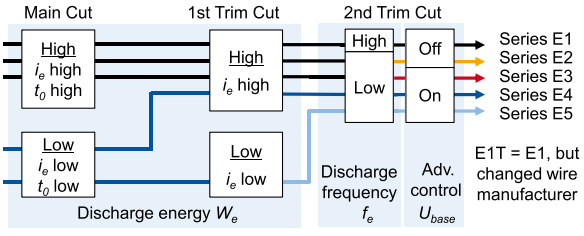

Fig. 2. Wire EDM manufacturing sequences for series E1–E5, E1T.

determine long-life fatigue (LLF) which is at the transition from the inflection point between low and high cycle fatigue. The LLF strength was determined by testing between 12 and 25 parts with the so called "staircase method" over $5 \bullet 10^6$ load cycles. Machining and testing details can be retrieved from [14]. The benchmarks (grinding and shot peening) were executed under turbomachinery industrial conditions under non-disclosure.

3. Wire EDM process monitoring

In Wire EDM a comprehensive knowledge of the influence of the individual process parameters is required to achieve specific goals concerning the machining productivity and the surface integrity of the workpiece [20]. Thus, Fig. 2 only represents a rough categorisation of the underlying much more detailed parameter sets used. All details can be found in [19]. Regarding the discharge current as key parameter, for the main cut i_e = 600 A was used for the high discharge energy setting and 350 A for the low setting. For the first trim cut i_e = 30 A (high W_e) and 15 A (low W_e) were used. For the second trim cut, the discharge current varied between i_e = 4–10 A.

To expand the insight into the interrelationships of the physical phenomena, the voltage and current signal data are combined to distinguish different types of discharges and analyse their spatial distribution. Based on single discharge experiments, a basic parameter set screening was executed. Normal and abnormal discharges were characterized based on the measured discharge energies and resulting craters. As resulting criterium for differentiation in the consecutive process, a lower limit of i_e = 300 A was defined for normal discharges compared to abnormal ones.

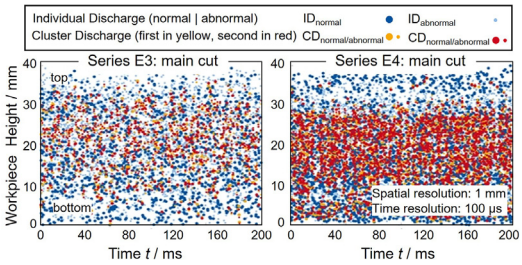

Fig. 3. Spatially resolved analysis of individual and cluster discharges.

Fig. 3 exemplarily shows the temporal and spatial distribution of occurring individual and cluster discharges of E3 and E4 main cut. As expected, the frequency of clusters increases with the discharge frequency of the main cut. Individual discharges in blue can be classified as normal discharges (dark blue) as well as abnormal discharges (light blue), see [19]. Yellow indicates the first discharges, red the subsequent discharges within clusters. In both series, the clusters occur most frequently in the two centre segments in which the removed particles accumulate due to reduced flushing [16]. For the top zone, a comparatively low number of normal discharges resulting in biggest workpiece crater sizes [19] can be identified for comparably best flushing condition. This deteriorates for the bottom position with changed discharge conditions due to wire wear.

Fig. 4 shows the resulting residual stresses (X-ray diffraction) for the reference series E3 after the second trim cut for the four clamping positions. Depth curves are available for the two centre clamping

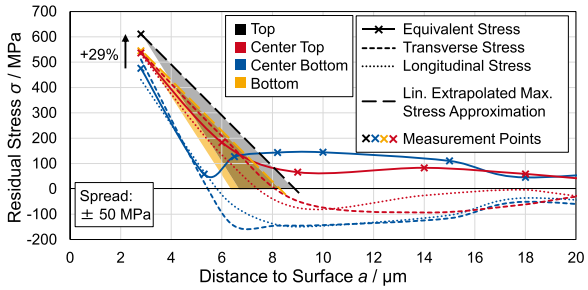

Fig. 4. Zone-based residual stress depth profile of E3 S trim cut.

positions, while the upper and lower clamping positions are each represented by a surface measurement. The difference between the top and centre bottom surface stress is just under 30%. The effects on the penetration depth of the residual stresses can be seen by comparing the depth curve of the two centre clamping positions, where the longitudinal and transverse stresses have dropped to zero at approx. 6 µm and 8 µm. Using linear extrapolation based on the zero-crossing difference, penetration depths can be estimated for bottom and top positions, which are around 9 µm in the maximum case [19].

Assuming that the spatially resolved characterisation of the discharge distribution, which can only be evaluated for the main cut due to an otherwise too low signal-to-noise ratio, can essentially be transferred phenomenologically to the subsequent trim cuts, the maximum value of the surface stress correlates closely with the absolute normal discharge frequency of occurrence in the height segments. The residual stresses therefore increase with the individual energy of the normal discharges coupled into the workpiece. Additionally, it can be assumed that cascade effects due to residual stress residues transferred from preceding cuts [21] are partly responsible for the measured surface stress differences. If the discharge frequency distributions described also prevail in the subsequent cuts, it can also be assumed that the residual stress variance is also systematically generated anew with each subsequent cut.

E1-E5 series generally show maximum tensile residual stresses between 400 and 530 MPa. Among these, the maximum surface stresses of E4 are the lowest at −12% compared to the basic technology E1. Those of the E5 series are the highest at +5% in the same ratio. Series E1T achieves the lowest value of all series at $\sigma_{V,E1T}$ = 403 MPa. The low residual stresses of E1T and E4 contradict the lower long-term strength of these series compared to the base technology (E1). The reasons for the later shown lower strength values are therefore to be found in unstable process control (E1T) or incomplete surface layer renewal (E4).

4. Bending fatigue results

In Fig. 5 the results of the LLF strength tests of the specimens machined by Wire EDM (E1-E5) are shown. Additionally, one series with an alternative wire electrode (E1T), a two-cut strategy – main and one trim cut – (2E) and a grinding reference (G) are shown, see also [14]. The change is represented in relation to the base parameter set E1. The mean (50%), 10% and 90% probability of failure L_{aL} are shown. The scattering margin T_L – i.e. the ratio of 90% and 10% probability of failure – provides a certain indication of the reproducibility of the production results.

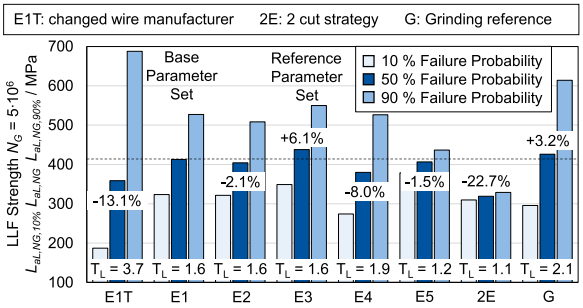

Fig. 5. Long life fatigue (LLF) of test series, based on [14].

The scattering range varies significantly, regardless of the average LLF strength achieved. While the changes in the second trim cut of E2 and E3 have no influence on the scattering range compared to E1, modifications in the main cut and first trim cut have both positive (E5) and negative effects (E4) regarding reproducibility. The smallest scattering range occurs in the two-cut process (2E), which emphasises the importance of the second trim cut and its adjustment for reproducible strength properties. The change of the wire tool for E1T shows the highest scatter range and thus illustrates the sensitivity of the process to external influences. The ground reference G has a higher scatter range than all wire technologies except for E1T [14].

For the mean LLF strength, only the from now on called reference parameter set E3 (+6.1%) and the ground series G (+3.2%) outperform the base parameter set E1. The series in which only the discharge frequency is reduced in the second trim cut E2 and the series with combined energy reduction of main cut and first trim cut E5 achieve a comparable level to E1. This shows that reducing the discharge frequency during the second trim cut is less effective than modifying the base voltage U_{base} in E3. The results of E5 show that a reduction of the discharge-related energy input in the main cut and first trim cut does not necessarily lead to a higher LLF strength. The mean LLF strength of E4 falls 8% behind the basic technology E1. The main reason for this is an unbalanced energy gradation [19].

As expected, omitting the second trim cut (2E) results in a significant reduction in LLF strength of over 22%. This series does not come close to achieving the required surface roughness (Ra_{2E} = 2.55 µm) and therefore fails earlier due to the greater notch effect and rim zone damage. The ground series G shows a 3.2% increase in LLF strength compared to E1. The increase is therefore lower than with the WEDM reference E3. In an earlier study of Welling the ground specimens achieved the same absolute level of mean LLF strength of just over 400 MPa that was also achieved in this work. However, his Wire EDM specimens showed an LLF strength about 45% worse than the results achieved in the present investigations [7,14]. This indicates that the use of latest generator and suitable engineering can raise component strength to the level of grinding.

E1-E5 all achieved a roughness on average below the specified limit [19] of Ra = 0.75 µm. There are occasional outliers in the E1, E1T and E5 series, whose maximum exceeds the specification by up to 0.03 µm. The ground series falls far short of the target roughness with an average arithmetic mean roughness value of Ra_G = 0.21 µm and was therefore machined 'too well'. Due to the height dependence of the Wire EDM process, the influence of the clamping position must be analysed.

Fig. 6a shows the variation of Ra for the specimens for the entire specimen spectrum (E1-E5, E1T) as a function of their height positioning within the clamping fixture. The average Ra increases in the wire run-off direction, while the scattering on the outer positions is increased compared to the centre positions. Because in the top segment the standard discharges show the highest individual removal, the roughness minimum there appears counter-intuitive at first. However, it is likely that melting and increased melt build-up due to incomplete removal occur more frequently in the centre segments due to the high particle loading there. This can result in pronounced roughness peaks. On the other hand, in the upper component area, into which runs unused wire, the electric field that determines the discharge location is almost exclusively constricted by the roughness peaks on the workpiece side during the trim cuts. This means that these can be removed effectively. The rougher the surface topography is created on the wire due to wear, the more this also determines the location of the strongest electric field. This reduces the effectiveness with which the highest roughness peaks are removed as the wire wear increases [19].

There is also a systematic correlation between the final specimen thickness and the clamping position, see Fig. 6b. The specimens clamped at the top show the smallest deviation from the target value of d = 3 mm, while the specimen thickness increases by a total of around Δd = 5 µm in the wire run-off direction. The scattering of the sample thicknesses also increases in the wire run-off direction. The obvious cause of this is the increasing wire wear, which could be reduced in a targeted manner by a technology-specific future readjustment. Certain effects due to flushing influences are also superimposed. Overall, it can be seen that the relative positioning of the samples in the fixture has an influence on dimensional accuracy and surface quality, with the uppermost position, where unused wire enters, having the highest dimensional accuracy and lowest roughness.

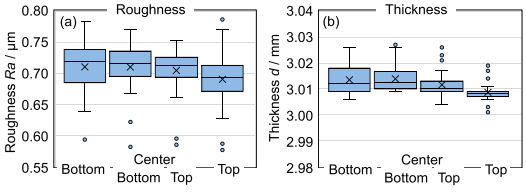

Fig. 6. Roughness Ra (a) and thickness d (b) by clamping position.

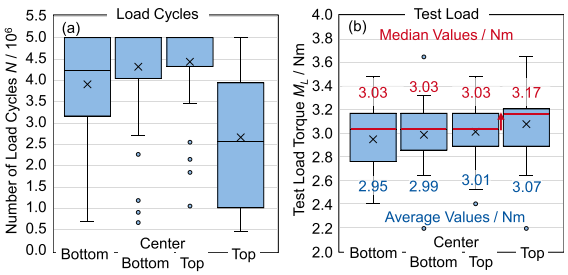

Fig. 7. Achieved cycles (a) and related load (b) by clamping position.

The effects of the clamping position on the number of cycles achieved are shown in Fig. 7a. When considering all series samples, it could be assumed that the average number of cycles achieved is similar for all positions. However, there are systematic differences. The specimens in the outer clamping positions achieve a lower average number of cycles than the centrally positioned specimens. The value for the top position is clearly the lowest. These specimens achieve the best dimensional accuracy and surface roughness but also exhibit the highest tensile residual stress. The specimens in the lowest position also break earlier than the centrally clamped ones. They exhibit the greatest roughness in the height comparison and show a medium tensile residual stress level.

Although the individual specimens were tested in random order during the test using the staircase method, it is necessary to check which mean test load torque corresponds to the number of cycles achieved in each case. This is shown in Fig. 7b. The mean value and median are relevant, as well as the scatter width upwards and downwards, as high loads reliably lead to fractures, while low loads lead to run outs. While the lower three positions have approximately the same mean values and, above all, the same median value, the mean value of the test load torque is one load level higher at the top position, which is at least a partial explanation for the lower number of cycles achieved [19].

To check whether there is a systematic influence of the specimen position independent of the load, the three most common load levels (3.17, 3.03 and 2.89 Nm) are each analysed separately. Here too, the medium specimens achieve higher cycle numbers in all load levels and that the top position in particular achieves the lowest mean cycles. For all load levels, the specimens that were clamped in top and bottom position were the most likely to fail. At a test load of 3.03 Nm, all specimens in position center bottom, and at 2.89 Nm all specimens in the center positions passed.

Fig. 8 finally shows the overall correlation between LLF and the main influencing factors surface roughness and residual stresses for the Wire EDM series and the grinding reference. In addition, two post-processes have partly been incorporated exemplarily representing a final shot peening (-SP) and stress relieving heat treatment (-HT) operation (see also [14]). The best results of the main subtractive processes Wire EDM (E3) and grinding G could still be increased. This is achieved by the pure reduction of the tensile residual stresses (-HT) or by the adding of compressive stresses while increasing the roughness in parallel (-SP).

There are clear interactions between roughness and residual stress state, which is why a joint linear regression between the input

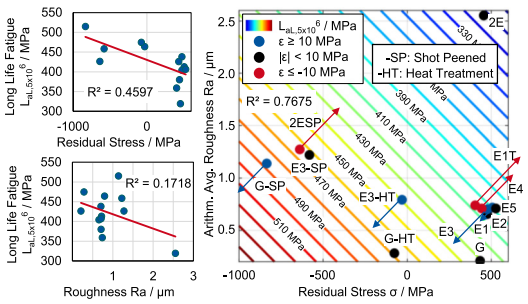

Fig. 8. Correlation of roughness and residual stress with LLF strength.

variables and the output variable LLF strength results in a better correlation coefficient than the separate correlation of the two characteristic values with the LLF strength [19]. The residual term ε of the linear regression is defined as the deviation vector showing the distance to the reference plane shown.

The achieved results of the plain geometries can qualitatively directly be transferred to more complicated geometries like fir trees. For Wire EDM no significant influence can be anticipated as the flushing conditions have already incorporated a distanced nozzle position. The absolute values cannot be directly used due to a possible superposition of notching effects of the geometry.

Both post-processes presented show a remaining potential of typical surface fatigue improvement techniques to be explored further in more detailed research approaches in the future. Besides the presented capabilities of shot peening and posteriori heat treatment, the potential of laser shock peening could be highly interesting from industrial application point of view.

5. Summary and conclusions

This work analysed the state-of-the-art Wire EDM machining of Inconel 718 parts regarding roughness and residual stresses. A spatially resolved analysis was conducted for main and trim cuts. Finally, the resulting long life bending fatigue performance was characterized in a zone resolved and overall analysis and compared to reference results of alternative machining approaches. Regarding Wire EDM process analysis the following can be stated:

- The spatially resolved process analysis revealed a changing distribution in number and characteristics of discharges for the main cut along the part height. The characteristics could be explained by the existing knowledge on process physics.
- A zone-based influence of the Wire EDM process on the resulting fatigue life along the workpiece height could clearly be shown and traced back to the spatially resolved discharges.
- A final post-processing by shot peening, which typically is done in industrial cases anyway, can still improve the overall dynamic part strength.

Future research activities should focus on the use of the full capacity of advanced generator technology and real-time adaptive EDM control to enhance dedicated local discharge distributions and to actively influence surface morphology and therefore the resulting part strength. Further activities could analyse the capabilities of advanced wire coatings, further hybrid process approaches and the setup of a fatigue prediction model.

Declaration of competing interest

The authors declare that they have no known competing financial interests or personal relationships that could have appeared to influence the work reported in this paper.

CRediT authorship contribution statement

Andreas Klink: Writing – review & editing, Writing – original draft, Visualization, Supervision, Project administration, Methodology, Funding acquisition, Formal analysis, Conceptualization. **Lukas Welschof:** Writing – review & editing, Writing – original draft, Visualization, Validation, Software, Methodology, Investigation, Formal analysis. **Kai Oßwald:** Writing – review & editing, Writing – original draft, Formal analysis, Visualization. **Tim Herrig:** Writing – review & editing, Supervision, Resources, Project administration, Data curation.

Acknowledgements

The work was funded by Deutsche Forschungsgemeinschaft DFG – 223500200–TRR 136 “Process Signatures”, project T01.

References

[1] Bergs T, Klocke F (2025) *Fertigungsverfahren 3 – Funkenerosion, elektrochemische Bearbeitung und Strahlverfahren*, Springer ViewegBerlin, Germany.
[2] Klocke F, Klink A, Veselovac D, Aspinwall DK, Soo SL, Schmidt M, Schilp J, Levy G, Kruth JP (2014) Turbomachinery component manufacture by application of electrochemical, electrophysical and photonic processes. *CIRP Annals - Manufacturing Technology* 63:703–726.
[3] Arrazola PJ, Rech J, M`Saoubi R, Axinte D (2020) Broaching: cutting tools and machine tools for manufacturing high quality features in components. *CIRP Annals - Manufacturing Technology* 69:554–577.
[4] Heidemanns L, Seelbach T, Küpper U, Seimann M, Bergs T (2021) Manufacturing technologies for fir tree slots: a technological and economic evaluation. In: *Proceedings of ASME Turbo Expo 2021*, GT2021–G59652.
[5] Aspinwall DK, Soo SL, Berrisford AE, Walder G (2008) Workpiece surface roughness and integrity after WEDM of Ti–6Al–4V and Inconel 718 using minimum damage generator technology. *CIRP Annals - Manufacturing Technology* 57: 187–190.
[6] Antar MT, Soo SL, Aspinwall DK, Sage C, Cuttell M, Perez R, Winn AJ (2012) Fatigue response of Udimet 720 following minimum damage wire electrical discharge machining. *Materials and Design* 42:295–300.
[7] Welling D (2014) Results of surface integrity and fatigue study of wire-EDM compared to broaching and grinding for demanding jet engine components made of Inconel 718. *Procedia CIRP* 13:339–344.
[8] Ayesta I, Izquierdo B, Flano O, Sanchez JA, Albizuri J, Aviles R (2016) Influence of the WEDM process on the fatigue behavior of Inconel 718. *International Journal of Fatigue* 92:220–233.
[9] Chen Z, Moverare J, Peng RL, Johansson S (2016) Surface integrity and fatigue performance of Inconel 718 in wire electrical discharge machining. *Procedia CIRP* 45:307–310.
[10] Holmberg J, Wretland A, Hammersberg P, Berglund J, Suarez A, Beno T (2021) Surface integrity investigations for prediction of fatigue properties after machining of alloy 718. *International Journal of Fatigue* 144:106059.
[11] Van Riel T, Qian J, Lauwers B (2024) Wire EDM roughing and Wire ECM finishing of 316L stainless steel on a single platform – An investigation of the combined strategy on surface quality and precision. *CIRP Annals – Manufacturing Technology* 73:109–112.
[12] Herrig T, Osswald K, Lochmahr I, Klink A, Bergs T (2020) Geometrical analysis of wire electrochemical machining for the manufacture of turbine disc slots. *Procedia CIRP* 95:694–699.
[13] Küpper U, Seelbach T, Heidemanns L, Prinz S, Herrig T, Bergs T (2022) Effects of the manufacturing chain on the surface integrity when machining fir tree slots with alternative manufacturing processes. *Procedia CIRP* 108:728–733.
[14] Welschof L, Wittenburg J, Petersen T, Herrig T, Klink A (2024) Bending fatigue performance due to different roughing-finishing sequences and post-processing of components produced by Wire EDM. *Procedia CIRP* 123:298–303.
[15] Boccadoro M, D'Amario RD, Baumeler M (2020) Towards a better controlled EDM: industrial applications of a discharge location sensor in an industrial wire electrical discharge machine. *Procedia CIRP* 95:600–604.
[16] Küpper U, Herrig T, Bergs T (2021) Visualization of spatially resolved energy in wire electrical discharge machining. *Procedia CIRP* 104:1512–1517.
[17] Küpper U, Tchoupe E, Klink A, Bergs T (2022) Prediction of geometrical accuracy in wire EDM by analyzing process data. *Procedia CIRP* 113:23–28.
[18] Küpper U, Klink A, Bergs T (2023) Data-driven model for process evaluation in wire EDM. *CIRP Annals – Manufacturing Technology* 72:169–172.
[19] Welschof L (2025) *Ermüdungsfestigkeit drahtfunkenerodierter Nickelbasiswerkstoffe für Triebwerksanwendungen = fatigue life of nickel-based alloys for turbine engine applications processed with wire electrical discharge machining*, Dissertation RWTH Aachen University. Accessed May 01, 2025. https://rwth-aachen.sciebo.de/s/fvG37BCm0GEeW6D.
[20] Maradia U, Filisetti E, Wiessner M, Schneider S, Boccadoro M (2020) The influence of energy input characteristics on surface integrity in wire EDM. *Procedia CIRP* 95:268–272.
[21] Osswald K, Klink A, Schneider S, Bergs T (2024) Residual stress effects of multiple thermal material loads due to a roughing-finishing sequence of electrical discharge machining processes. *Procedia CIRP* 123:232–237.